

## SIMULATION ANALYSIS ON THE TESTING DEVICE OF FOUR-COMPONENT BOREHOLE STRAIN METER IN THE UNDERGROUND

Jie-Ning XIA<sup>1,2,3</sup>, Li-Xia GENG<sup>1,2,3</sup>, Zhen LI<sup>1,2,3</sup>, Song LUO<sup>1,2,3</sup>, Nong-Fa  
LI<sup>1,2,3</sup>

*In this paper, a test scheme of four-component borehole strain meter in the underground is proposed, and simulation analysis is creatively used to verify the feasibility of the pre-processing testing device to verify the feasibility of the scheme. Through the simulation analysis of the displacement of the testing device, the working mechanism of the testing device is simulated, and the relationship between the displacement of the exciting device and the deformation of the external wall of the borehole strain meter sensor is understood. At the same time, the mechanical characteristic of the sensor and the transmission loss is analyzed. The simulation analysis of the radial stiffness and frequency response characteristics of the strain sensor proves that the device can be used to test the linearity, resolution, range and frequency range of the four-component strain meter.*

**Keywords:** Underground, Borehole Strain meter, Testing device, ANSYS, Simulation analysis

### 1. Introduction

Surface deformation and tectonic movement in the interior of the crust and its various geo-hazards are closely related to the effect of the crustal stress; the change of crustal stress state is the most direct cause of fracture, folds and even the earthquakes [1]. Exploring the crustal stress state and its law of action is one of the important ways to understand the physical process of the earth's interior and study the mechanisms of earthquake and geo-hazards.

Borehole strain meter is the main instrument used to measure the state of stress and strain in the internal stratum. Its probe is usually installed in bedrock (or soil) tens of meters below the borehole [2][3]. The strain precursor of earthquakes as well as the distribution and development after earthquakes are mastered by observing the strain state of internal strata changing with time.

---

<sup>1</sup> Hubei Key Laboratory of Earthquake Early Warning, Institute of Seismology, China Earthquake Administration, Wuhan, China

<sup>2</sup> Hubei Key Laboratory of Earthquake Early Warning, Hubei Earthquake Agency, Wuhan, China

<sup>3</sup> Wuhan Institute of Seismologic Instrument Co., LTD, Wuhan, China

Email: 23028186@qq.com

However, the actual output of observation data is often affected by a variety of factors, including human activities, instrument failures, meteorological changes and many unknown factors. Especially for the instrument, the underground borehole strain meter with complex structure and special installation method (it cannot be moved after a single installation), which brings great difficulties to demonstration of the structural scheme, test and calibration of the instrument. With the increasing demand for the instrument market, mass production is imperative. How to test and calibrate the performance index of the borehole strain meter is a very practical technical problem [4] [5]. This paper presents a better index scheme. Meanwhile, the simulation method is used for early analysis and verification, which greatly simplifies the experiment process and shortens the verification cycle of the program.

## 2. Test scheme of the borehole strain meter

The probe structure of four-component borehole strain meter (SKZ-3 XIANG-YANG KONG et al.) is shown in Fig.1. The radial displacement capacitance sensors are  $45^\circ$  with each other in four directions, which is used to detect the change of the inner diameter of the cylinder caused by in-situ stress. The change of borehole diameter causes the change of capacitance polar distance, and then the change of capacitance. The measuring circuit converts the change of capacitance into electrical signal and transmits it to the ground through signal cable.

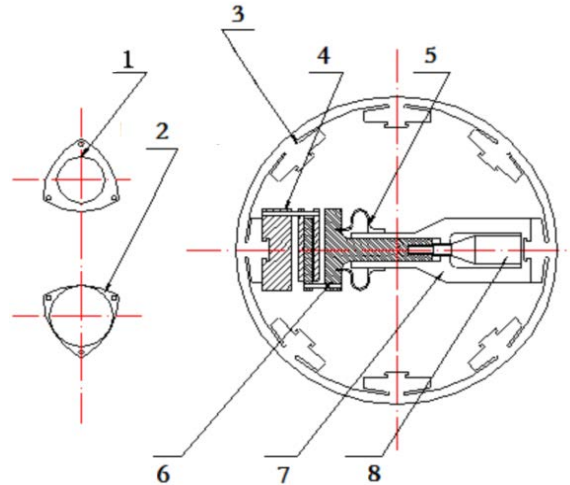


Fig.1 Mechanical structure of sensor

1. rotor plate of capacitance 2. stator plate of capacitance 3. feeling cylinder of sensor 4. pole of stator plate 5. stable plate 6. pole of rotor plate 7. guide cylinder 8. mobile zeroing device

According to the technical requirements of seismic monitoring network instruments in the Seismic Industry Standard of People's Republic of China (DB/T 31.2, 2008), at least the resolution, range, linearity and frequency range should be tested. Taking linearity test as an example, the testing method and the required equipment are explained in detail.

## 2.1 Test method of linearity

- a) The displacement is inputted to the probe of strain meter by high-precision piezoelectric ceramics, and the output displacement of piezoelectric ceramic changes equally to 10% of the full range of the probe.
- b) The least square method is used to fit the curve:

$$y_i = a + bx_i \quad (1)$$

where,  $x_i$  is the given displacement of piezoelectric ceramic and  $y_i$  is the fitting value of voltage.

The average value is  $\bar{x} = \frac{\sum_{i=1}^n x_i}{n}$ ;  $\bar{y} = \frac{\sum_{i=1}^n y_i}{n}$ ,  $n$  is the measuring point number.

The calculation formula of each coefficient:

$$a = \bar{y} - b\bar{x}, \quad b = L_{xy}/L_{xx};$$

$$L_{xx} = \sum_{i=1}^n (x_i - \bar{x})^2, \quad L_{xy} = \sum_{i=1}^n (x_i - \bar{x})(y_i - \bar{y})$$

- c) A linear deviation is,

$$\Delta y_i = y_i - Y_i \quad (2)$$

where, the maximum deviation in the set of  $(\Delta y_i)$  is  $\Delta y_{\max}$ ;  $Y_i$  represents the actual voltage output measured by multimeter corresponding to  $x_i$ , and the linearity is:

$$\delta = \frac{\Delta y_{\max}}{\Delta y_{FS}} \times 100\% \quad (3)$$

where,  $\Delta y_{FS}$  represents the full range output of the measuring value of voltage.

## 2.2 Testing device and connection diagram

Connection diagram of the testing device is shown in Fig. 2. The test process requires a stress on the piezoelectric ceramics. Micro-displacement measuring screw and capacitance sensor inside the strain meter synchronously record the deformation of the outer cylinder, and a test cylinder is also needed to fix these devices. Among them, the closed-loop piezoelectric ceramics adopt

RA150 series with high accuracy and internal displacement as well as self-correcting at present.

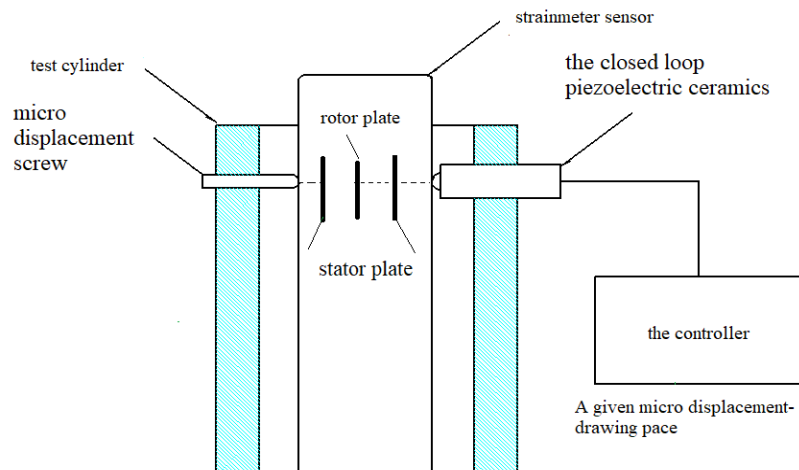


Fig.2 Connection diagram of linearity test equipment

In the process of linearity testing, it is a key problem to ensure the accuracy of stress transfer and the expected linearity testing effect of the whole set of testing devices. The author's team first proposed that the strain meter probe should be placed in a thick-walled stainless-steel test tube, and quartz sand should be buried to simulate the working state of the strain meter to test the noise. After testing, it was found that quartz sand landfill site could not stabilize the probe of strain meter and the noise test results were not satisfactory. The other scheme is to use a closed-loop piezoelectric ceramics to give micro-displacement in the direction of strain meter sensing. Another scheme is to use closed-loop piezoelectric ceramics to give micro-displacement in the direction of strain meter sensing. At the same time, a micro-displacement sensor is installed on the same side of the closed-loop piezoelectric ceramic device to monitor the actual deformation of the strain meter when the closed-loop piezoelectric ceramics are given a displacement. According to the test results, it is found that the mechanical transfer loss and insufficient rigidity exist in the extrusion strain meter sensor wall of the closed-loop piezoelectric ceramics testing device. The measured displacement produced by the closed loop piezoelectric ceramics is not the actual deformation of the external wall of the strain meter sensor. Therefore, a micro-displacement screw sensor is also needed to measure the actual deformation of the outer wall, which is used to compare the deformation with the measured value of the capacitance sensor, thus the test scheme of strain meter linearity formed is shown in Fig.2. However, there would be more problems in the actual

testing process, such as what is the suitable wall thickness, where the micro-displacement screw should be to better reflect the real value, whether the overall testing device would affect the linearity test and more. Similarly, the measurement of resolution, range and frequency range also needs matching test devices. Thereby, how to constantly adjust the details constantly to find the most reasonable schemes, it would cost a lot of manpower and material resources it is determined by real experiment; on this basis, we consider breaking the conventional way of simulation design simulation design.

### 3. Simulation analysis

First, it is necessary to simulate the operating mechanism and working process of the testing device, as well as to understand the relationship between the displacement of piezoelectric ceramics and the external wall of strain meter so as to analyze the mechanical transmission loss [6-8].

#### 3.1 Simulation analysis of displacement test

##### Analysis model

A finite element analysis model is established [9][10] according to structure of the testing device shown in Fig. 3. The simulation model is composed of a test device (simplified as a test pass) 2 and a strain meter sensor 1.

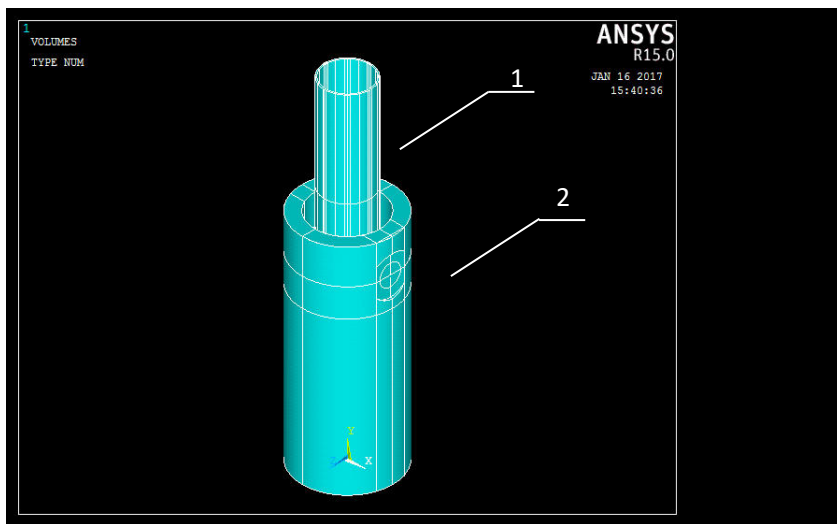


Fig.3 Finite element analysis model of the testing device (1) strain meter sensor (2) testing device

According to the structure of the test device and sensor, the simulation model is simplified as follows without affecting the results.

a) Only one pair of capacitance plates is built in the strain meter sensor. The hemispherical shape with a radius of 3 mm in the front section of the piezoelectric ceramic stack (see 1 in Fig.4) is simplified to the cylinder with a diameter of 1mm and 3mm, and the stiffness is assumed to be the maximum.

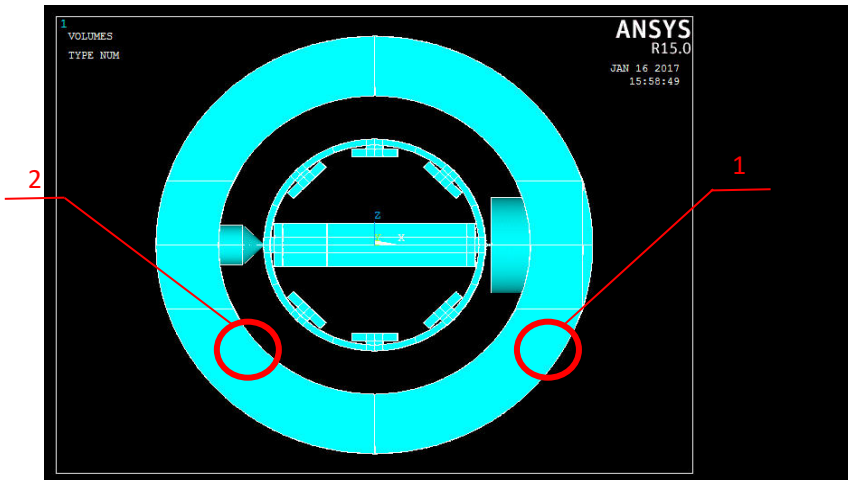


Fig.4 The simplified schematic diagram of piezoelectric displacement exciter model

b) The 10mm radius hemisphere in the front of the pin M20 at the other fixed end (see 2 in Fig. 2) is simplified to a cone.

c) The contact area between both sides of the front end and sensor is a line segment of 1mm in length.

d) The initial distance between the plates is set to 50 microns.

e) The plate circle is simplified to square.

### Calculation parameters and constraints

According to the design, the testing device and the left fixed end pin are made of No.45 steel. Piezoelectric stack sheets at 1 in Fig.4 are rigid and the modulus of elasticity is set to  $1e10$ MPa (about  $2.1e5$ MPa for conventional steel). The material of the strain meter is stainless steel. Since the whole plate is a non-solid structure, its density is equivalent to  $2e-3$ g/mm<sup>3</sup>.

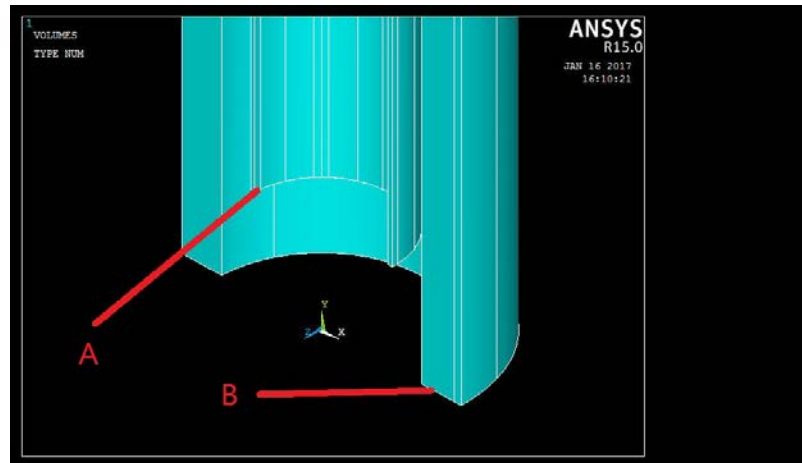


Fig.5 The constrained boundary conditions of sensors and test device

Fig. 5 is the constrain diagram of the simulation model. Sensor A only constrains the vertical direction (Y). Fixed constraints (x, y, z all constraints) are applied to the B-plane of the test device.

The displacement boundary conditions with relative displacement of 0.2 micron are applied to the cylinders with diameter of 1 mm and length of 3 mm (see 1 and 2 in Fig. 4) in front of piezoelectric ceramic stacks (see 1 in Fig. 6).

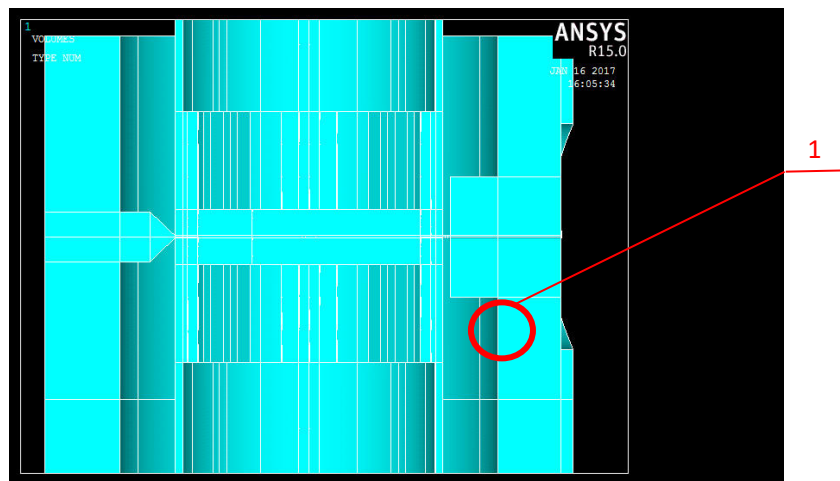


Fig.6 The position diagram of displacement excitation

### Calculation Results and Analysis

When the driving displacement of the test device is 0.2 microns, the finite element simulation results of the test device and sensor are shown in Fig.7 to Fig.

11 respectively. The displacement of the model in radial direction (X direction) is represented by color cloud pictures with mm.

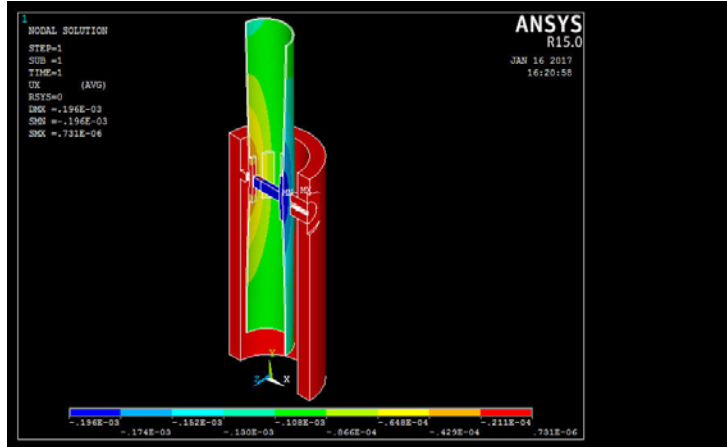


Fig.7 Displacement cloud at x direction (Global)

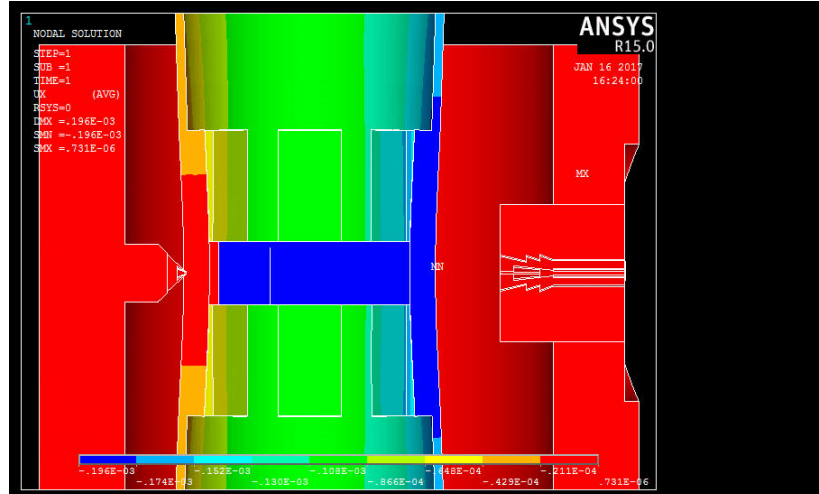


Fig.8 Displacement nephogram in x direction (Section view)

The displacement nephogramss of Fig.7 and Fig. 8 show that when the testing device is excited to 0.2 microns, the maximum displacement of the strain meter sensor occurs at the contact point with the testing device. The actual displacement of the sensor is less than 0.2 microns, only 0.196 microns, which is caused by the deformation on the other side of the sensor. The maximum displacement of the test device is only 0.731 nanometer, which is three orders of magnitude different from the driving displacement of 0.2 microns. The influence of the deformation of the testing device is negligible for the calibration result.

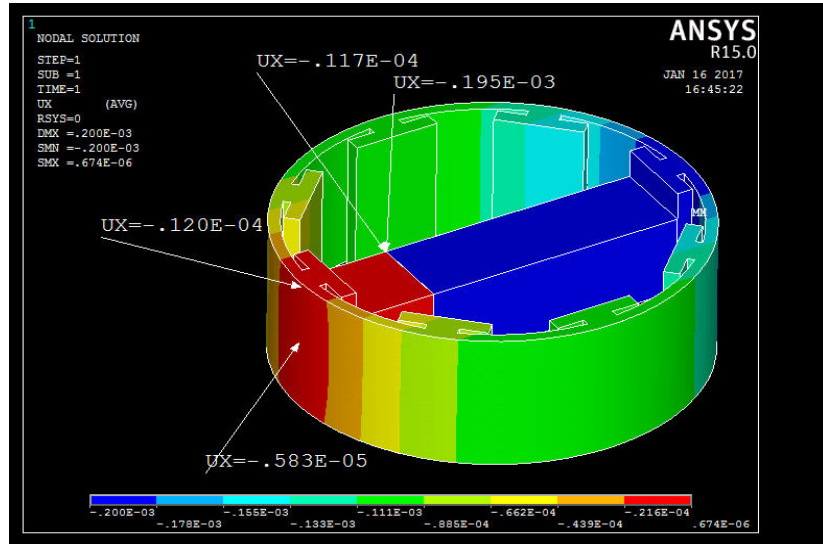


Fig.9 Displacement nephogram in x direction (Section view of plate)

Fig. 9 is the local radial displacement cloud after cutting from the plate along the radial direction of strain meter sensor. Fig.9 shows that under the excitation of 0.2 microns, the absolute displacement of the left polar plate (short side) is  $0.117\text{e-}4\text{mm}$  and the right plate (long side) is  $0.195\text{e-}3\text{mm}$ . The variation of the polar distance of the strain meter sensor under the excitation of 0.2 microns  $\Delta\delta = (0.195\text{e-}3) - (0.117\text{e-}4) = 0.183\text{e-}3\text{mm}$  can be calculated, which is less than 0.2 micrometers. The displacement at the fixed end of the thimble is  $0.583\text{e-}5\text{mm}$ , and  $0.12\text{e-}4\text{mm}$  at about 30mm above the thimble, which indicates that the non-driven thimble deforms the outer wall of the strain meter sensor deform (shown in Fig. 8).

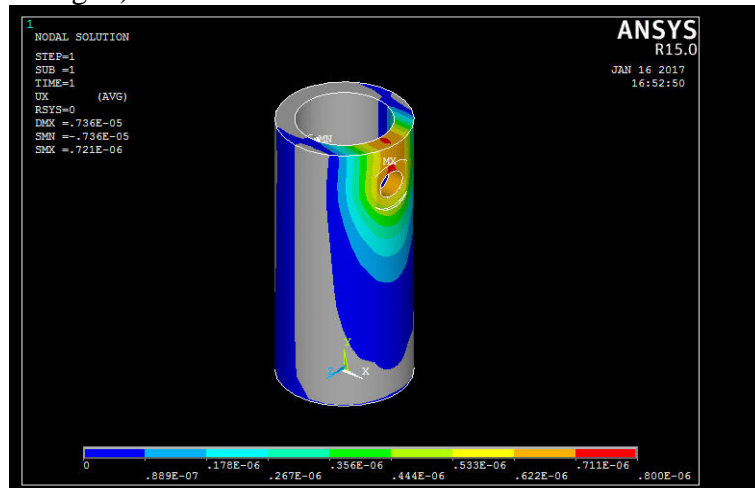


Fig.10 X direction deformation of the shell at the piezoelectric ceramic driver side

Fig. 10 is a radial (x-direction) deformation cloud of the test device. Fig.10 shows the deformation at the driving side of the piezoelectric ceramics in the test device mainly appears in the local area of the piezoelectric ceramics. The closer to the excitation device of piezoelectric ceramic and the greater the deformation. The maximum deformation is 0.73e-6mm, or 0.73nm. The maximum deformation is 0.73e-6mm, or 0.73nm.

Fig. 11 is a radial (x-negative) deformation cloud of the test device. Fig. 11 is a radial (x-negative) deformation cloud of the test device. From Fig.11, the deformation of the shell on the fixed pin side of the test device is very small with about 0.1e-6mm, while the larger part of the deformation is the tip of the pin. The local elastic deformation of the thimble occurs and the maximum deformation is about 0.3e-5mm.

From the above analysis, it can be seen that the deformation of the testing device is nanometer, the maximum deformation occurs in the driving side of piezoelectric ceramic, which is about 0.73 nm. The deformation is far less than the calibrating minimum displacement of 0.2 micron, which can be neglected. Therefore, the wall thickness of the current test device is appropriate.

When the displacement input is 0.2 micron, the polar distance conversion of the capacitor plate is less than 0.2 micron , which is 0.183 micron. The main reason for the deviation is that the thimbles in the fixed end and strain meter sensor of the testing device both produce radial deformation at the contact points. In order to reduce the deviation, the contact area between the fixed end thimble and the strain meter sensor can be increased, the deformation of the sensor shell can be reduced and the calibration accuracy can be improved. For the actual testing device, piezoelectric ceramics are standard part that has been purchased well, and the fixed end thimble is not good enough to change again. Considering that the radial deviation is relatively fixed, and the actual reading of the micro-displacement screw sensor is not the piezoelectric ceramic reading, which is compared with the capacitance sensor of the strain meter in the testing process, the deviation is acceptable in the allowable range of the error in the actual test.

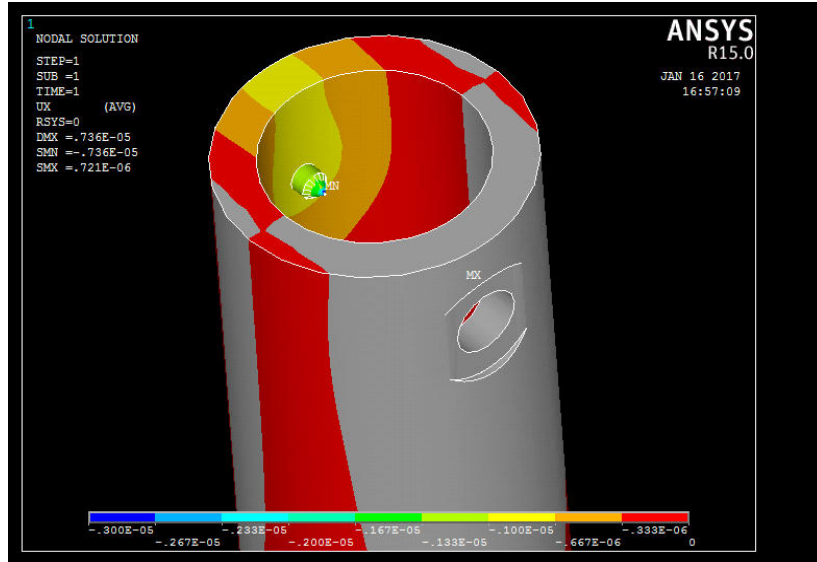


Fig.11 X direction deformation of the shell in the fixed end

### 3.2 Radial stiffness analysis of the strain meter

The radial stiffness of strain meter can also be simulated and analyzed to further confirm the rationality of the test scheme.

Using the same finite element model, the displacement excitation at the tip of the piezoelectric actuator is modified to force excitation. Add-x direction force on the sensor and X direction force on the test device respectively. The force increases from 1N to 10N with a step size. The z direction constraint is added to the contact point between the test device and strain meter sensor. The cross-section where the contact point is located is taken as the object of analysis, and the node of value is the node with positive center on two sides of the plate. The relationship between strain meter sensor and capacitance pole distance is shown in Table 1. From Table 1, it can be seen that the radial displacement of strain meter sensor is linear with the stress in the elastic range. The formula for calculating the radial stiffness of strain meter sensor is as follows:

$$K = \frac{F}{\Delta\delta} \quad (4)$$

Where,  $F$  is the force applied on the sensor;  $\Delta\delta$  is the distance change of the sensor, that is sensor deformation.

As shown in Table 1, the stiffness of strain meter sensor in x direction is 7310N/mm.

Table 1

The calculation results of sensor stiffness

$F(N)$	displacement at left end(mm)	displacement at right end(mm)	interval change $\Delta\delta$ (mm)	Stiffness(N/mm)
1	-8.13E-06	-1.44E-04	1.36E-04	7.35E+03
2	-1.63E-05	-2.89E-04	2.73E-04	7.33E+03
3	-2.45E-05	-4.34E-04	4.10E-04	7.32E+03
4	-3.26E-05	-5.79E-04	5.47E-04	7.31E+03
5	-4.08E-05	-7.24E-04	6.84E-04	7.31E+03
6	-4.90E-05	-8.69E-04	8.21E-04	7.31E+03
7	-5.72E-05	-1.01E-03	9.58E-04	7.31E+03
8	-6.53E-05	-1.16E-03	1.10E-03	7.31E+03
9	-7.35E-05	-1.30E-03	1.23E-03	7.31E+03
10	-8.17E-05	-1.45E-03	1.37E-03	7.30E+03
Average value of the stiffness				7.31E+03

### 3.3 Simulation analysis on frequency response of the strain meter

Because the frequency bandwidth test of strain meter requires different frequency excitation signals from piezoelectric ceramics, the frequency response of strain meter sensor can be analyzed by simulation analysis method first.

The displacement excitation at the tip of the piezoelectric actuator is modified to alternating force on the basis of the finite element analysis model of the stiffness analysis on the original strain meter sensor. The force amplitude is selected as 240N and the frequency range is from 0Hz to 300Hz. The other boundary conditions remain unchanged and harmonic response analysis is carried out for the model. Taking three nodes of the long side plate as the object of analysis, the frequency response curves of the three nodes are shown in Fig. 12.

From Fig. 12, it can be seen that the maximum excitation frequency at the extreme end of the plate is about 250-270Hz, which is far beyond the frequency band set by the instrument itself, with the range of 100HZ. The strain meter sensor tends to be stable for the frequency response characteristics of the excitation source. The frequency range of the instrument can be tested through the testing device.

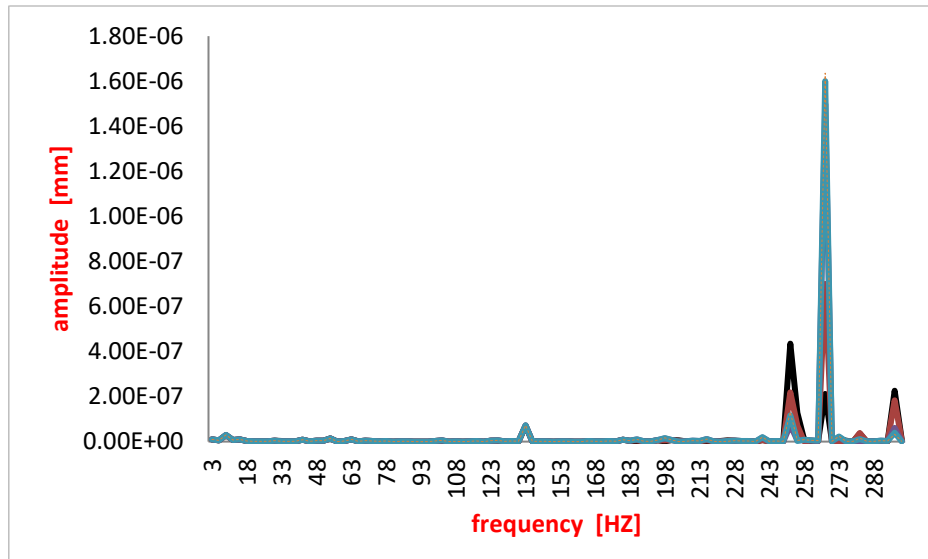


Fig.12 The frequency response curve of plate displacement

#### 4. Conclusion

The simulation results show that, there is a slight deviation between the displacement input generated by the test device and the distance transform of the capacitance. Considering that the radial deviation is relatively fixed, and the actual reading of is not the readings of the piezoceramic, which is compared with the capacitance sensor of the strain meter in the testing process, the deviation is acceptable in the allowable range of the error in the actual test. At the same time, the radial stiffness of the sensor is obtained by simulation calculation, and the frequency response of the strain meter sensor is analyzed by simulation analysis method. It is conclusion that the frequency response of strain meter sensor to excitation source tends to be stable in the range of 100HZ.

In a word, the design of the test device is reasonable, and the stability is optimal. It can better transmit the excitation signal to the measured target sensor in the range of error. The ratio of test results of target strain meter sensor to the measured value of the micro displacement sensor can better achieve the key indications test of the underground four-component borehole strain meter. In the design phase of the test scheme, the simulation analysis method saves a lot of manpower and material resources and the simulation results are accurate, which is also verified by the actual measurement. The simulation analysis method is worth popularizing and applying.

## R E F E R E N C E S

- [1]. Anfu Niu, Yilin Wu, Defu Chen, Xiaojun Li, The Datong earthquake and its anomalous tilt Field, *Acta Seismologica Sinica (English Edition)*, **vol.** 4, 1995, pp. 615-620.
- [2]. *Canitano A, Hsu Y J, Lee H M, et al.*, Calibration for the Shear Strain of 3-component Borehole Strain meter in Eastern Taiwan through Earth and Ocean tidal Waveform Modeling, *Journal of Geodesy*, **vol.** 3, 2017, pp.1-18.
- [3]. *ZehuaQiu, Lei Tang, Longshou Zhou, et al.* Observed Strain Changes From 4-complonet Borehole Strain meter Network before 2008 Wenchuan Earthquake, *Journal of Geodesy and Geodynamics*, **vol.** 29(1), 2009, pp.1-5.
- [4]. *ZehuaQiu, Yaolin Shi, Zuxi Ouyang*. Relative In-situ Calibration of 4-component Borehole Strain Observation, *Journal of Geodesy and Geodynamics*, **vol.** 25(1) 2005, pp.118-122.
- [5]. *Lixin Wu, Liqiang Zhang, Guobin Li, et al.* The relative calibration and data application of 4-component borehole Strain observation in Haiyuan. *Journal of Seismological Research*, **vol.** 33(4), 2010, pp. 318-322.
- [6]. *Feifei Liu, Fengchong Lan, Jieqing Chen*. Simulation and experiment of vehicle Li ion power battery temperature field based on dynamic internal heat source characteristics. *Chinese Journal of Mechanical Engineering*, **vol.** 52(8), 2016, pp. 141-151.
- [7]. *Ling Ai, Yi Zhu, Ye San*. Numerical simulation of temperature field of the environment simulation system in ultra deep well underground. *Journal of Harbin Institute of Technology*, **vol.** 47(1), 2015, pp. 61-67. 2015
- [8]. *Korotkov A S, Loboda V V, Makarov S B, et al.* Modeling thermoelectric generators using the ANSYS software platform: Methodology, practical applications, and prospects. *Russian Microelectronics*, **vol.** 46(2), 2017, pp. 131-138.
- [9]. *Tomar V P S, Dwivedi D*. ANSYS simulation of temperature distribution in plate casting. *Development*, **vol.** 2(9), 2015
- [10]. *Reddy K A, Reddy T V S, Satpagiri S*. Heat Flux and Temperature Distribution Analysis of IC Engine Cylinder Head Using ANSYS. *International Journal of Advanced Research Foundation (IJARF)*, **vol.** 2(5), 2015, pp. 21-26.